CO₂ capture performance of Ca-Mg acetates at realistic Calcium Looping conditions

Juan Miranda-Pizarro[a,b], Antonio Perejón[a,c,*], Jose Manuel Valverde[b], Luis A. Pérez-Maqueda[a], Pedro E. Sánchez-Jiménez[a]

[a]Instituto de Ciencia de Materiales de Sevilla (C.S.I.C.-Universidad de Sevilla). C. Américo Vespucio 49, Sevilla 41092. Spain.

[b]Faculty of Physics, University of Seville, Avenida Reina Mercedes s/n, 41012 Sevilla, Spain.

[c]Departamento de Química Inorgánica, Facultad de Química, Universidad de Sevilla, Sevilla 41071, Spain.

*Corresponding author:

antonio.perejon@icmse.csic.es

Instituto de Ciencia de Materiales de Sevilla (CSIC-Universidad de Sevilla).

C. Américo Vespucio 49, Sevilla 41092. Spain

Tel. (+34) 95 448 95 00

Fax (+34) 95 446 01 65

CO₂ capture performance of Ca-Mg acetates at realistic Calcium Looping conditions

Juan Miranda-Pizarro[a,b], Antonio Perejón[a,c], Jose Manuel Valverde[b], Luis A. Pérez-Maqueda[a], Pedro E. Sánchez-Jiménez[a]

[a]Instituto de Ciencia de Materiales de Sevilla (C.S.I.C.-Universidad de Sevilla). C. Américo Vespucio 49, Sevilla 41092. Spain.

[b]Faculty of Physics, University of Seville, Avenida Reina Mercedes s/n, 41012 Sevilla, Spain.

[c]Departamento de Química Inorgánica, Facultad de Química, Universidad de Sevilla, Sevilla 41071, Spain.

Abstract

The Calcium Looping (CaL) process, based on the cyclic carbonation/calcination of CaO, has emerged in the last years as a potentially low cost technique for CO_2 capture at reduced energy penalty. In the present work, natural limestone and dolomite have been pretreated with diluted acetic acid to obtain Ca and Ca-Mg mixed acetates, whose CO_2 capture performance has been tested at CaL conditions that necessarily imply sorbent regeneration under high CO_2 partial pressure. The CaL multicycle capture performance of these sorbents has been compared with that of CaO directly derived from limestone and dolomite calcination. Results show that acetic acid pretreatment of limestone does not lead to an improvement of its capture capacity, although it allows for a higher calcination efficiency to regenerate CaO at reduced temperatures (~900ºC) as compared to natural limestone (>~930ºC).

On the other hand, if a recarbonation stage is introduced before calcination to reactivate the sorbent, a significantly higher residual capture capacity is obtained for the Ca-Mg mixed acetate derived from dolomite as compared to either natural dolomite or limestone. The main reason for this behavior is the enhancement of carbonation in the solid-state diffusion controlled phase. It is argued that the presence of inert MgO grains in the mixed acetate with reduced segregation notably promotes solid state diffusion of ions across the porous structure created after recarbonation.

1. Introduction

The Calcium-Looping (CaL) process is being widely investigated in the last years as a potential solution to capture CO_2 from energy intensive industries such as coal fired power plants [1-2]. The process is based on the reversible carbonation/calcination of CaO solids in two interconnected fluidized bed reactors using low cost (~10\$/ton), widely available, non-toxic natural limestone (close to 100% $CaCO_3$) as CaO precursor [3-5]. CO_2 from the flue gas stream is captured in the carbonator reactor by chemical reaction of CaO with CO_2 after which the carbonated solids are circulated into a second fluidized bed reactor (calciner) where CaO is regenerated by calcination, which releases a concentrated CO_2 stream to be compressed, transported and stored or employed in other uses [3, 6-7]. Conditions of the CaL process for post-combustion capture involve short residence times and gas velocities of a few m/s in both reactors. The concentration of CO_2 in the carbonator is around 15% vol. as typical of flue gas, and the optimum working temperature is around 650ºC. In the calciner, CaO regeneration and calcination of the fresh limestone makeup must take place under CO_2 at high concentration (70-90% vol.), which requires operation at temperatures above 930ºC. Calcination at high temperatures under high CO_2 partial pressure is a drawback for integrating the CaL process into industrial plants. On one hand, it poses an energy penalty for the technology [8-9]. On the other, it causes a marked aggregation and sintering of the CaO nascent grains during the $CaCO_3$/CaO transformation, which leads to a drastic decrease of the CaO surface area available for quick carbonation in a subsequent cycle [10-11]. As demonstrated in previous studies [12], carbonation of CaO particles takes place through two different phases. The first phase is controlled by reaction kinetics until a $CaCO_3$ layer is built upon the surface of the particle, after which carbonation becomes ruled by the solid-state counter-current diffusion of ions across this product layer. The short residence times

100 employed for carbonation in the CaL process is thought to limit the CO_2 capture

101 efficiency in practice to the fast reaction phase at the surface of the particles [13]. In order

102 to mitigate the drastic loss of CaO activity, it has been proposed to introduce a

103 recarbonation stage between the carbonation and calcination stages [14-15]. The

104 operation temperature of the recarbonator would be around 800ºC, and CO_2 concentration

105 should be high in order to accelerate carbonation in this intermediate stage (~90% vol.).

106 Calcination of the recarbonated solids would yield a CaO skeleton with enhanced porosity

107 and therefore higher carbonation activity in short residence times.

108 The trade between cost of the Ca-based sorbent and its CO_2 capture capacity is a critical

109 issue for scaling up this technology to an industrial level [16]. Natural limestone is the

110 main candidate to be used at large-scale due to its wide availability, non-toxicity and low

111 price [3-4, 17-19]. Yet, the fast deactivation rate of limestone derived CaO (lime) has

112 sparked research on synthetic materials, such as CaO-based sorbents modified with

113 organic acids to produce calcium acetate, calcium propionate or calcium citrate among

114 others [16, 20-24]. Li et al. reported promising results from CO_2 capture tests using

115 calcium magnesium acetate [25]. The sorbent derived from dolomite treated with acetic

116 acid showed indeed a superior multicycle conversion behavior as compared with CaO

117 directly derived from dolomite calcination (dolime) under the same experimental

118 conditions. The role of MgO on improving the conversion behavior of Ca-Mg synthetic

119 sorbents for CO_2 capture has been widely investigated in previous works. Thus, it has

120 been observed that calcium acetate and carbide slags sintering is mitigated by the addition

121 of small amounts of MgO [26-28]. Other authors have employed commercial calcium

122 magnesium acetates with diverse calcium to magnesium molar ratios and found that CaO

123 conversion was enhanced as the magnesium content was increased [29]. Wet mixing

124 combustion synthesis has been also employed to prepare sorbents with diverse amounts

125 of Mg [30]. Coprecipitation is another technique that has been used to prepare synthetic

126 Ca-rich dolomites, with high and stable CaO conversion [31]. However, calcination

127 conditions play a crucial role on the behavior of Ca-based sorbents when subjected to

128 CaL cycles [32-33]. To the best of our knowledge, CaO sorbents derived from calcium

129 and calcium magnesium acetates have been mostly tested under mild calcination

130 conditions involving low CO_2 partial pressure environments. Yet, realistic CaL conditions

131 for CO_2 capture necessarily involve calcination under high CO_2 partial pressure.

132 This work is focused on the investigation of the multicycle CO_2 capture behavior of CaO

133 derived from calcium acetate and calcium magnesium acetate at CaL conditions implying

134 sorbent regeneration under high CO_2 partial pressure.

135

136

137 **2. Materials and methods.**

138 The materials employed in this work were natural limestone received from Segura S.L.

139 (Matagallar quarry, Pedrera, Spain) of high purity (99.6%wt $CaCO_3$) and natural dolomite

140 from Bueres quarry (Asturias, Spain). The predominant phase (94.4% wt.) of dolomite is

141 $CaMg(CO_3)_2$, with the rest being $CaCO_3$ (~5%) plus impurities (<1%).

142 Acetic acid of high purity (99.9%) from VWR Chemicals (CAS: 64-19-7) was used to

143 prepare the acetates.

144 As a first step, limestone and dolomite were precalcined in a muffle furnace at 900ºC for

145 2 hours in air to obtain the corresponding oxides. CaO derived from limestone and

146 CaO·MgO from dolomite calcination were treated with diluted acetic acid (50% vol. in

147 aqueous solution), at the rate of 8.1 g per 140 mL for CaO and 8.5 g per 120 mL for

148 CaO·MgO. Then, the mixture was magnetically stirred at room temperature for 24 hours

149 and dried at 120ºC.

150   The instrument used to perform the carbonation/calcination and

151   carbonation/recarbonation/calcination multicycle tests was a thermogravimetric analyzer

152   (TGA) Q5000IR from TA Instruments. The instrument is equipped with an infrared

153   halogen lamp furnace. Four lamps are placed symmetrically with respect to a SiC

154   enclosure, which allows for fast heating/cooling transitions (300ºC/min). In CO_2 capture

155   applications, the solids are rapidly circulated between the reactors; therefore, the

156   transition between stages in TGA tests must be fast in order to mimic realistic conditions.

157   Otherwise, a slow transition from carbonation to calcination would lead to a prolonged

158   carbonation of the sorbent that would critically affect its multicycle behavior. The TGA

159   instrument is also equipped with a high sensitivity balance (<0.1 µg), characterized by a

160   minimum baseline dynamic drift (<10 µg). A thermocouple positioned close to the sample

161   underneath it registers the temperature during the cycles.

162   The conditions employed in this work consist of a precalcination stage carried out by

163   increasing the temperature (300ºC/min) up to 900ºC under 30% air/70% CO_2 vol/vol.

164   atmosphere. Carbonation/calcination (carb/cal) tests are initiated by quickly decreasing

165   the temperature for carbonation at 650ºC under typical flue gas conditions (85% air/15%

166   CO_2 vol/vol.). Then, the sample is calcined by increasing again the temperature up to

167   900ºC under 30% air/70% CO_2 vol/vol. As will be seen, an advantage of the use of Ca

168   and Ca-Mg acetates is that calcination is efficient in short residence times under this

169   reduced temperature as compared to limestone, which requires calcination temperatures

170   above 930ºC to achieve full decarbonation in short residence times [1]. Residence times

171   of 5 minutes for both calcination and carbonation stages have been used as typical

172   reference times at practical conditions. In the experiments in which a recarbonation stage

173   was introduced after carbonation, it was carried out for 3 minutes at 800ºC under 90%

174   CO_2/10% air (vol/vol). The mass employed for testing the multicycle behavior of the

7

175 different materials was ~5.5 mg with the objective of avoiding undesired effects caused

176 by poor mass transfer phenomena and gas diffusion resistance through the samples [34].

177 Scanning Electron Microscopy (SEM) micrographs were taken using an ultra-high

178 resolution HITACHI S5200 instrument. X-Ray diffractograms were acquired in the 2θ

179 range from 5º to 90º using a Panalytical X'Pert Pro diffractometer working at 45 kV and

180 40 mA with CuKα radiation, and equipped with an X'Celerator detector and a graphite

181 diffracted beam monochromator.

182

183

184 **3. Results and discussion.**

185 **3.1. Acetic acid pretreatment of natural limestone and dolomite.**

186 Figure 1 shows the X-ray diffraction patterns registered for limestone and dolomite after

187 being treated with the diluted acetic acid solution.

188 As may be seen in Figure 1a, the main Bragg reflection peaks observed for modified

189 limestone correspond to partially hydrated Ca acetate. A minor peak indicates the

190 existence of a quite small amount of Ca-Mg acetate produced by the presence of MgO

191 impurities in the raw limestone [35-36]. On the other hand, the reflection peaks observed

192 for modified dolomite (Figure 1b) correspond to Ca-Mg acetate, with a secondary, but

193 non negligible, phase of Ca acetate [36], which will be referred to hereafter as Ca-Mg
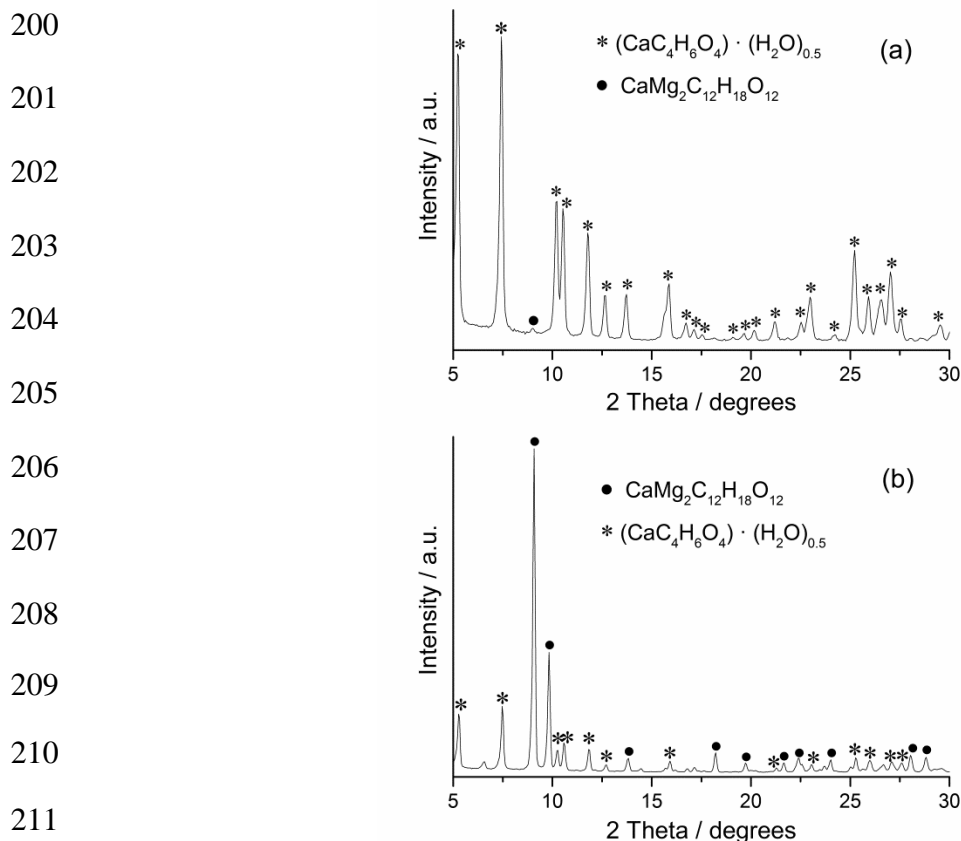
194 mixed acetate.

195

196

197

198

199

200
201
202
203
204
205
206
207
208
209
210
211

Figure 1. X-ray diffraction patterns of limestone (a) and dolomite (b) used in our experiments after pretreatment with diluted acetic acid.

Thermal decomposition of these Ca and Ca-Mg mixed acetates was studied by thermogravimetry. Figure 2 shows the thermograms obtained by heating the samples from room temperature to 950ºC at 10ºC min^{-1} in an air flow of 50 cm^3 min^{-1}. As may be seen, Ca acetate (Ca(CH$_3$COO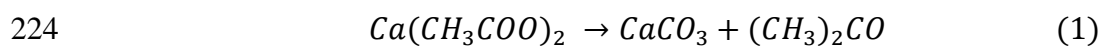)$_2$) decomposes mainly in three steps. In the first one (about 5% mass loss), dehydration takes place at temperatures between 134ºC and 201ºC. The second mass loss (around 35% of the total mass) occurs from 360ºC to 417ºC, whereby the decomposition of Ca(CH$_3$COO)$_2$ in CaCO$_3$ and acetone ((CH$_3$)$_2$CO) occurs via the reaction:
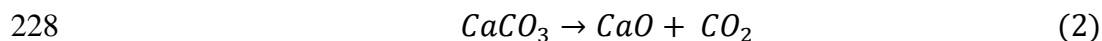
$$Ca(CH_3COO)_2 \rightarrow CaCO_3 + (CH_3)_2CO \qquad (1)$$

225 Finally, the last mass loss (26%) takes place in the range from 620ºC to 728ºC due to the

226 calcination of $CaCO_3$ to yield CaO:
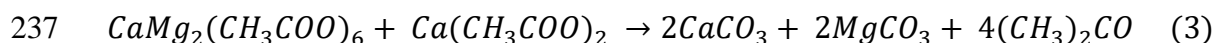
227

228 $$CaCO_3 \rightarrow CaO + CO_2 \qquad (2)$$

229

230 Figure 2b shows the thermal decomposition of the Ca-Mg mixed acetate obtained from

231 natural dolomite. The relatively important presence of Ca acetate yields some deviations

232 over the mass loss expected for pure Ca-Mg acetate. Thus, the mass loss in the first stage

233 (2%) corresponds to dehydration at temperatures from 138ºC to 194ºC. Afterwards, the

234 decomposition of the mixture of acetates in the corresponding carbonates and acetone

235 takes place between 326ºC and 427ºC (40% mass loss):

236

237 $$CaMg_2(CH_3COO)_6 + Ca(CH_3COO)_2 \rightarrow 2CaCO_3 + 2MgCO_3 + 4(CH_3)_2CO \quad (3)$$

238

239 In previous works, it has been proposed that decomposition of Ca-Mg acetate yields the

240 corresponding amounts of Ca and Mg carbonates as separate byproducts [37]. In our case

241 however, the co-existence of Ca acetate has to be taken into account in the stoichiometry

242 of the process (reaction 3). Between 430ºC and 460ºC decomposition of $MgCO_3$, which

243 has lower thermal stability than $CaCO_3$, takes place:

244

245 $$MgCO_3 \rightarrow MgO + CO_2 \qquad (4)$$
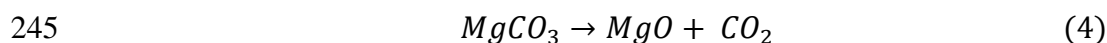
246

247 In the last decomposition phase, whereby about 10% of the total mass is lost, $CaCO_3$

248 decomposes in the temperature range from 611ºC to 686ºC. A 33% of the initial mass

249 remains after full decomposition is achieved, which corresponds to a mixture of CaO and

250 MgO (Figure 2b).
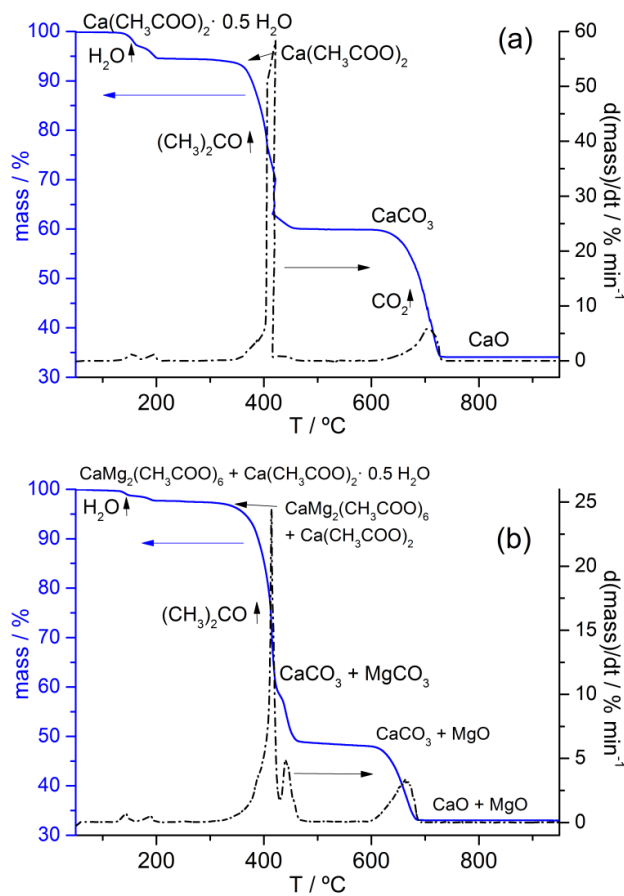
251

Figure 2. Temperature evolution of mass (% of initial mass) and its time derivative (right axis) during thermal decomposition of (a) Ca acetate and (b) Ca-Mg mixed acetate obtained from limestone and dolomite pretreated with diluted acetic acid, respectively (heating rate 10ºC min^{-1} under air).

3.2. Scanning electron microscopy analysis (SEM)

The microstructure of the Ca acetate and the Ca-Mg mixed acetate derived from limestone and dolomite, respectively, before and after the multicycle tests was analyzed by SEM. Micrographs of both acetates are shown in Figure 3. As can be seen, the samples exhibit the characteristic rod-shape grains of these acetates [38-41]. Note also how these rods are thinner for the Ca-Mg mixed acetate.

11

275

276

277

278

279

280

281

282

283

284

285
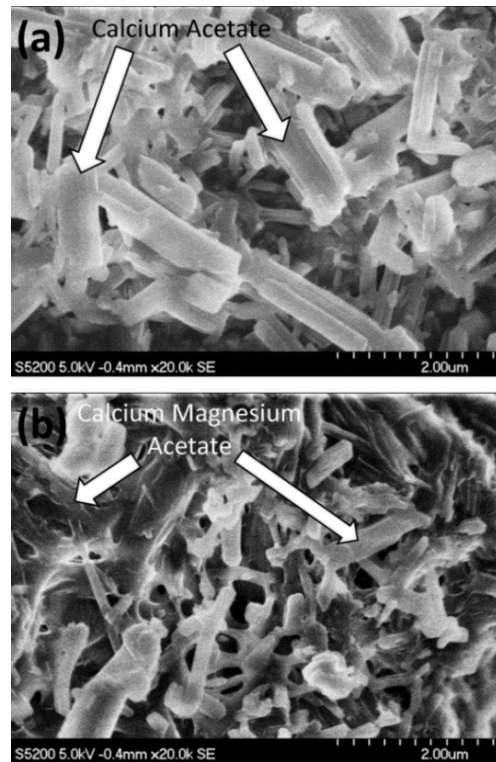
286 Figure 3. SEM micrographs of (a) limestone and (b) dolomite modified with acetic acid.

287

288 SEM micrographs obtained for the acetates after being subjected to multicycle

289 calcination/carbonation tests (as detailed in section 3.3) are shown in Figure 4. Figure 5

290 presents SEM micrographs of the sorbents after the cycles in which a recarbonation stage

291 was introduced between carbonation and calcination. The cycled Ca acetate typically

292 presents fissures, large pores and marked sintering of the CaO grains. On the other hand,

293 the cycled sample of the mixed Ca-Mg acetate shows a higher porosity. CaO grains in

294 this sample are of typically smaller size compared to those observed for the cycled Ca

295 acetate and can be clearly distinguishable from the MgO grains. The latter remain inert to

296 carbonation under the CaL conditions used in our tests and would presumably help

297 mitigating aggregation and sintering of the CaO grains as inferred from previous works

298 for natural dolomite [17, 42]. It is thus foreseeable that the capture capacity of the Ca-Mg

299 mixed acetate is improved as compared to Ca acetate.
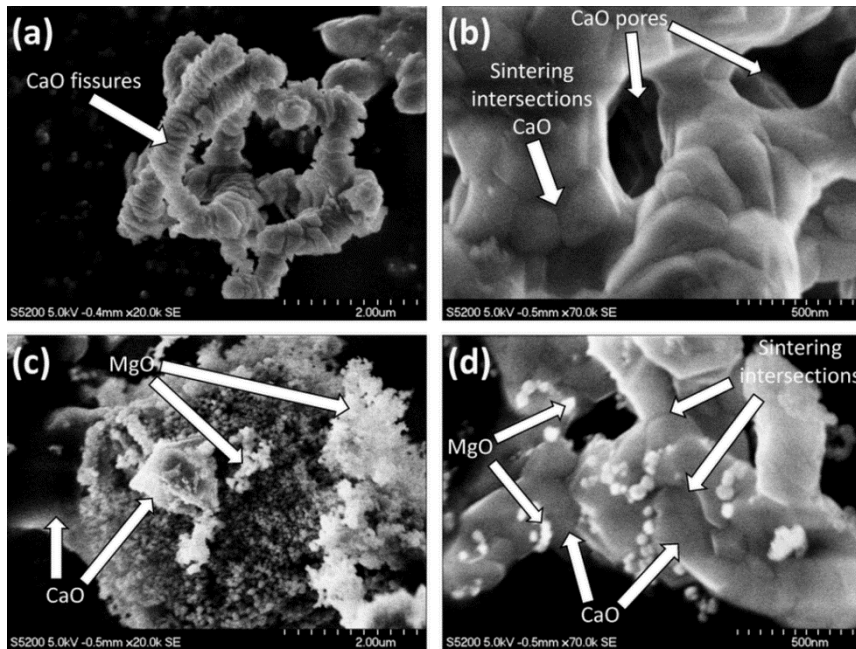
Figure 4. SEM micrographs of (a, b) Ca acetate and (c, d) Ca-Mg mixed acetate after 20 cycles consisting of 5 minutes carbonation at 650ºC (15% CO_2/85% air vol/vol) and 5 minutes calcination at 900ºC (70% CO_2/30% air vol/vol).
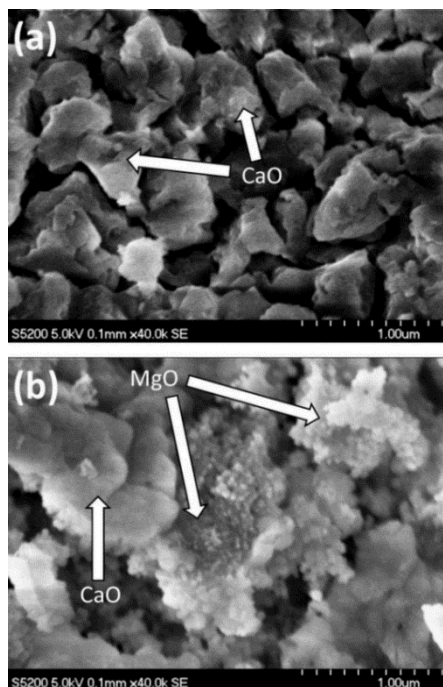
Figure 5. SEM micrographs of (a) Ca acetate and (b) Ca-Mg mixed acetate samples after 20 carbonation/recarbonation/calcination cycles. Carbonation at 650ºC (15% CO_2/85% air vol/vol) for 5 minutes, recarbonation at 800ºC (90% CO_2/10% air vol/vol) for 3 minutes, and calcination at 900ºC (70% CO_2/30% air vol/vol) for 5 minutes.

3.3. CO₂ capture capacity

Figure 6 shows the multicycle calcination/carbonation thermograms obtained for Ca acetate and the Ca-Mg mixed acetate. As can be seen, complete decomposition of the CaO precursors is achieved from the 1st calcination at 900°C under a 70% CO_2/30% air vol/vol atmosphere. This is a substantially lower temperature than the minimum temperature needed to achieve full calcination of natural limestone in short residence times (over 930°C) [17]. Thus, as a first important result it may be inferred that the use of acetates would allow operating the calciner at a reduced temperature compared to natural limestone, which would allow for a reduction of the energy penalty [1, 8-9].
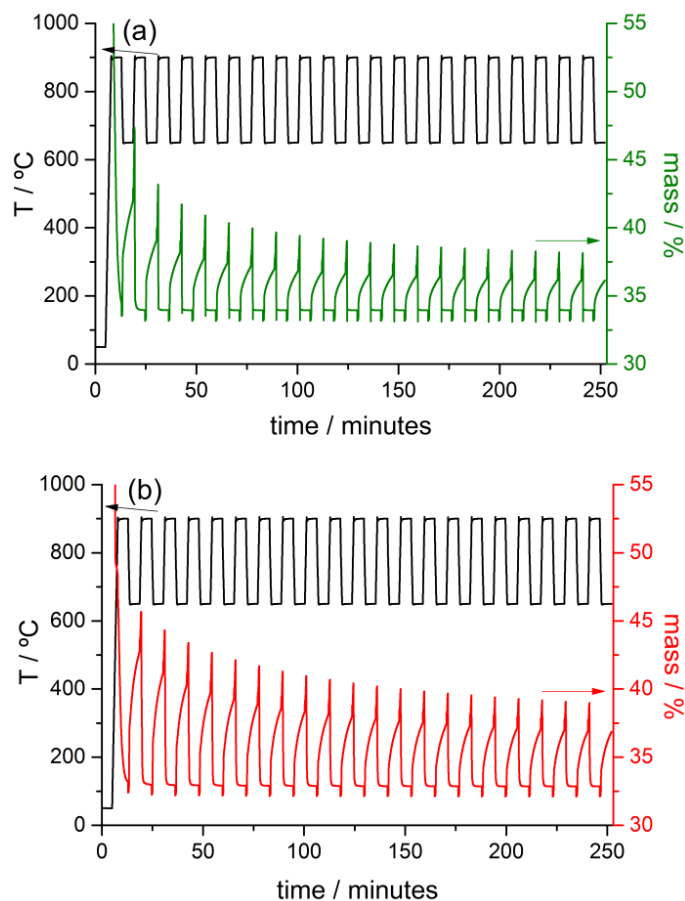
Figure 6. Time evolution of temperature and mass % during calcination/carbonation cycles measured by thermogravimetric tests on samples of Ca acetate (a) and Ca-Mg mixed acetate (b). Carbonation at 650°C (15% CO_2/85% air vol/vol) for 5 minutes and calcination at 900°C (70% CO_2/30% air vol/vol) for 5 min. Precalcination at 900°C (70% CO_2/30% air vol/vol) for 5 min.

14

This behavior suggests that the $CaCO_3$ formed in the second decomposition step of calcium acetate and calcium magnesium acetate is less crystalline than natural limestone, which favors decarbonation at reduced temperatures as seen in previous works for limestone and dolomite samples mechanically milled to reduce crystallinity [43]. With the objective of confirming this hypothesis, calcium acetate was decomposed at 500ºC to yield $CaCO_3$ and the XRD pattern was registered to compare it with that of natural limestone measured in the same conditions. In Figure 7 the main XRD reflections for both samples are shown. It is clear that, although the peak widths are similar, the peak intensities for $CaCO_3$ obtained from calcium acetate are smaller than for limestone. This indicates that calcium acetate derived $CaCO_3$ has a significantly lower crystallinity than limestone, which favors decarbonation.
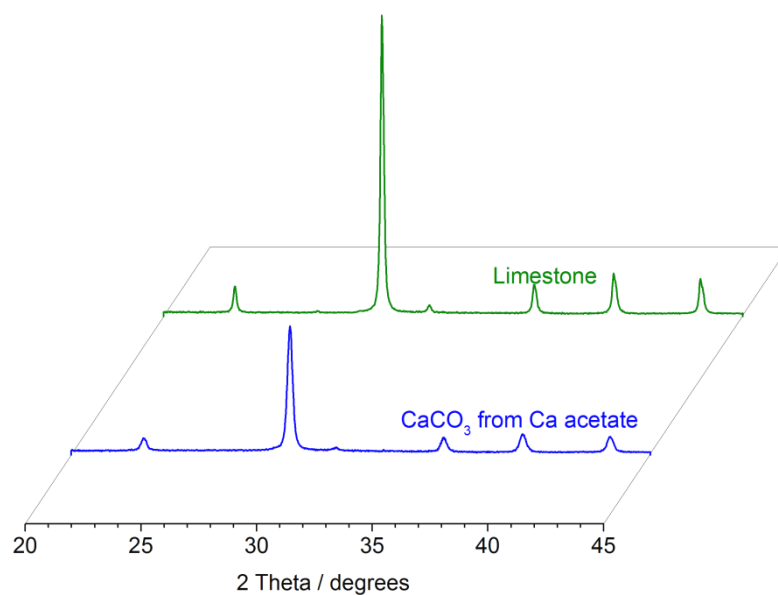

Figure 7. X-ray diffraction patterns obtained for natural limestone and $CaCO_3$ derived from Ca acetate decomposed at 500ºC.

377 The parameter used to compare the multicycle performance of the sorbents analyzed in

378 our work is their capture capacity, which takes into account the presence of compounds

379 inert to carbonation such as MgO in the sorbents derived from dolomite. The capture

380 capacity is defined as the mass gained during carbonation (mass of CO_2 captured in this

381 stage) divided by the mass of sorbent before carbonation was started. As can be observed

382 in Figure 6, the mass gained during the carbonation stages for the acetate derived from

383 dolomite (Figure 6b) is remarkably higher than for the acetate derived from limestone

384 (Figure 6a), which indicates a superior capture performance of this sorbent as will be

385 discussed in more detail below.

386 Multicycle capture capacity data for the Ca acetate are shown in Figure 8. Results are

387 compared with data obtained for CaO directly derived from natural limestone calcination

388 (in this case the minimum calcination temperature to achieve full decomposition from the

389 first cycle was 950ºC). As can be seen in Figure 8a, the capture capacities measured for

390 the Ca acetate are clearly below those obtained for natural limestone. The introduction of

391 a recarbonation stage (Figure 8b) when testing the Ca acetate leads to slightly higher

392 values of the capture capacity in the first cycles, albeit also clearly below those

393 corresponding to natural limestone. Therefore, it may be concluded that the acetic acid

394 pretreatment on limestone does not lead to an improvement of its multicycle capture

395 performance under realistic CaL conditions, which is a consequence of the marked

396 sintering of CaO derived from calcium acetate, as observed in Figures 4a, 4b and 5a.

397 Nevertheless, a reduction of the calcination temperature can be achieved, which would

398 serve to mitigate the energy penalty in the integration of the CaL process into a power

399 plant to be carefully assessed by heat integration analysis [44].

400

401
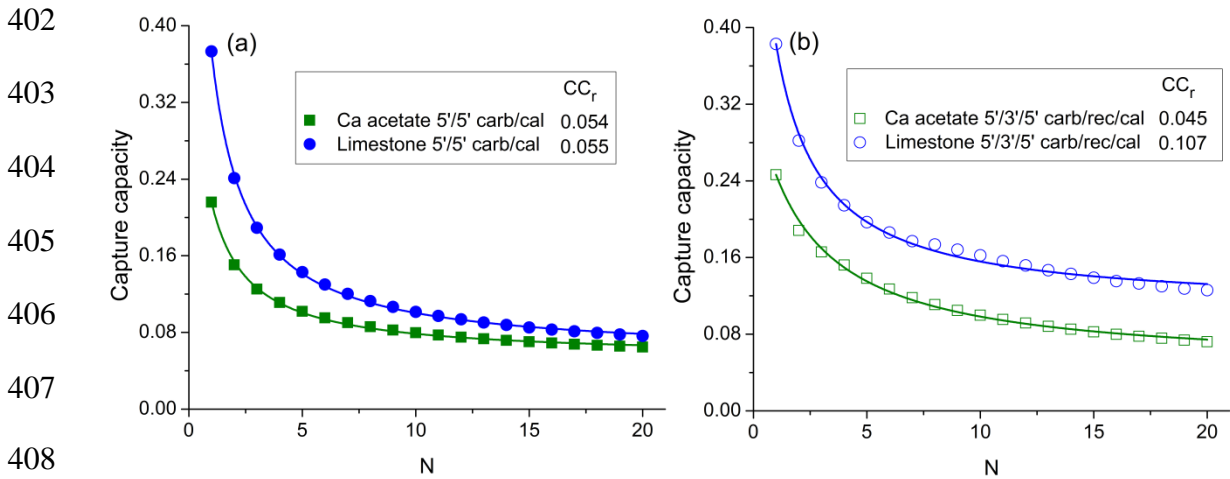
Figure 8. a): Capture capacity versus carbonation/calcination cycle number for CaO samples derived from Ca acetate and natural limestone. Precalcination at 900ºC (70% CO2/30% air vol/vol) for 5 minutes, carbonation (carb) at 650ºC (15% CO_2/85% air vol/vol) for 5 minutes, and calcination (cal) at 900ºC (70% CO_2/30% air vol/vol) for 5 minutes (in the case of limestone calcinations are carried out at 950ºC). b) Data from tests in which a recarbonation (rec) stage was introduced (90% CO_2/10% air vol/vol for 3 min at 800ºC) between the carbonation and calcination stages. The solids lines are the best fit curves of Equation (5) to experimental data (values of the residual capture capacity obtained from these best fits are shown in the inset).

As for Ca acetate, calcination of the Ca-Mg mixed acetate was fully achieved at 900ºC in short residence times (Figure 6b), which was thereby used also as calcination temperature for sorbent regeneration. Multicycle capture capacity data obtained for the Ca-Mg mixed acetate are plotted in Figure 9, where results on the capture capacity of the sorbent derived from natural dolomite calcination are also shown for comparison. As may be observed, the capture capacity curve of the Ca-Mg mixed acetate is slightly below that of natural dolomite (Figure 9a). On the other hand, the introduction of the recarbonation stage is in this case seen to mitigate substantially the deactivation of CaO derived from the mixed acetate (Figure 9b). Thus, the values of capture capacity for this sorbent are higher from

17

428   the 7th cycle as compared to those obtained for the sorbent directly derived from natural

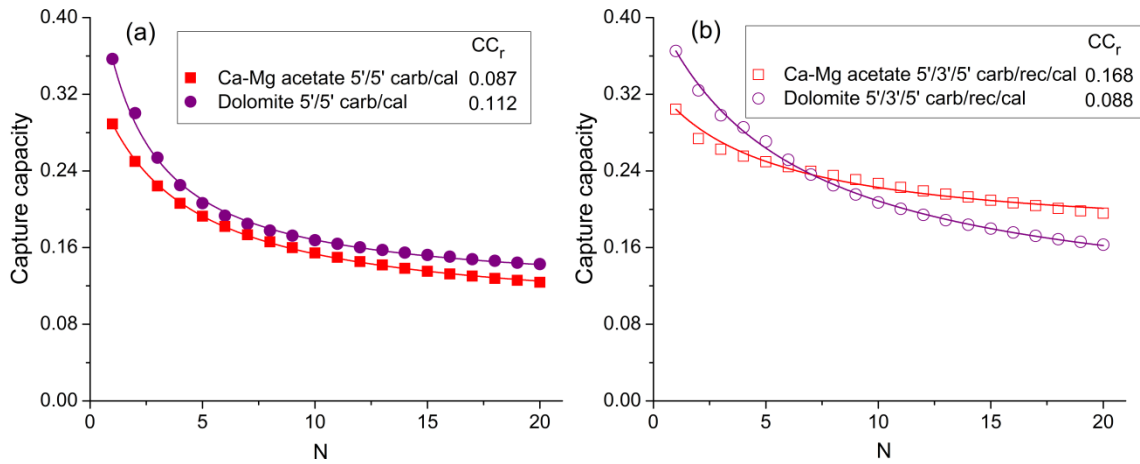429   dolomite calcination when a recarbonation stage is introduced.

430

431

438   Figure 9. Capture capacity data versus carbonation/calcination cycle number for sorbents derived

439   from the Ca-Mg mixed acetate and natural dolomite. Carbonation at 650ºC (15% CO2/85% air

440   vol/vol) for 5 minutes and calcination at 900ºC (70% CO2/30% air vol/vol) for 5 minutes. A

441   recarbonation at 800ºC (90% CO2/10% air vol/vol) for 3 minutes is introduced in b). The solids

442   lines are the best fit curves of Equation (5) to experimental data (values of the residual capture

443   capacity obtained from these best fits are shown in the inset).

444

445

446   Multicycle capture capacity data obtained from the TGA tests were fitted using the semi-

447   empirical equation [11, 45-46]:

448

450
$$CC_N = CC_r + \frac{CC_1}{k(N-1) + (1 - CC_r/CC_1)^{-1}}; \qquad (N = 1, 2 \dots) \qquad (5)$$

449

451   where N is the cycle number, CC_1 is the capture capacity at the first cycle, CC_r is the

452   residual capture capacity, towards which the capture capacity converges asymptotically

453 after a very large number of cycles, and k is the deactivation rate constant. As may be

454 seen, in Figures 8 and 9, Eq. (5) fits quite well to experimental data, which allows us to

455 infer a value of the residual capture capacity for the different sorbents tested (Table 1 and

456 insets of Figures 8-9). From these values, it can be concluded that the treatment with

457 acetic acid may lead to an improvement of the multicycle CO_2 capture performance but

458 only for natural dolomite and under carbonation/recarbonation/calcination cycles. In this

459 case a relatively high residual capture capacity is obtained ($CC_r = 0.168$), which is about

460 twice the value obtained for natural dolomite.

461

462 Table 1. Residual capture capacity (CC_r) values for CaO derived from calcination of Ca acetate,

463 natural limestone, Ca-Mg mixed acetate and natural dolomite.

|	Carb. (min)	Recarb. (min)	Calc. (min)	CC_r
Ca acetate	5	--	5	0.054
	5	3	5	0.045
Limestone	5	--	5	0.055
	5	3	5	0.107
Ca-Mg acetate	5	--	5	0.087
	5	3	5	0.168
Dolomite	5	--	5	0.112
	5	3	5	0.088

464

465

466

3.4. Relative role of fast-reaction and solid-state diffusion controlled carbonation phases

Figure 10 shows the time evolution of the capture capacity during the 20th carbonation for the sorbents analyzed in this work. Carbonation of CaO proceeds through two differentiated phases. Under carbonation at 650ºC, a fast reaction-controlled (FR) stage occurs first until a carbonate layer of about 30-50 nm thickness is built on the surface of the particles [47-48]. The FR phase is followed afterwards by a relatively slower phase, which is governed by the counter-current solid-state diffusion (SD) of O^{2-} and CO_3^{2-} ions across the product layer [49]. Figure 10 shows also that a great part of the overall capture capacity is due to carbonation in the SD phase when sorbent regeneration is carried out under high CO_2 partial pressure according to practical conditions, which contrasts with most of previous observations from tests in which calcination was performed under low CO_2 partial pressure [50].
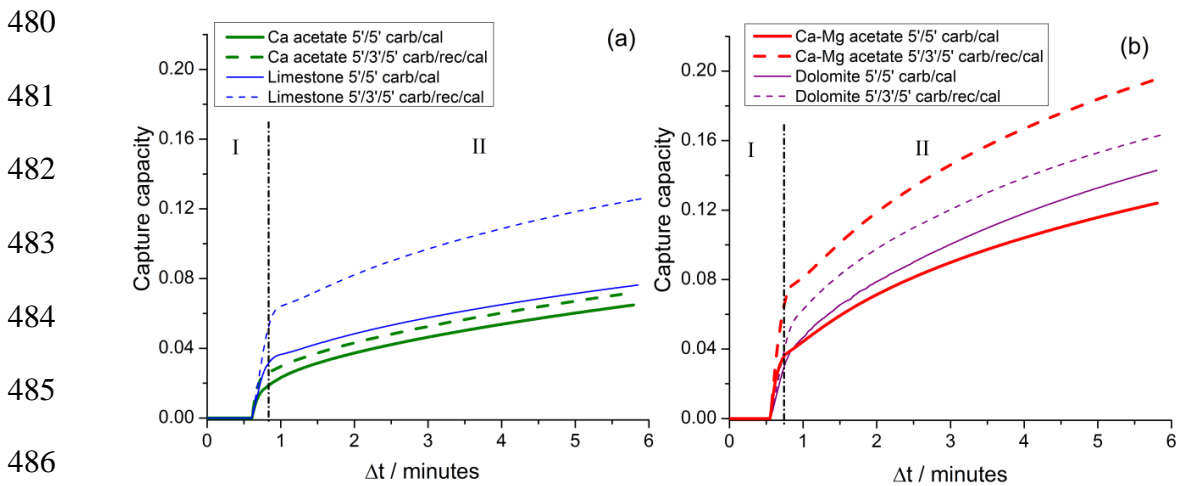
Figure 10. Time evolution of CO_2 capture capacity during the 20th cycle for (a) Ca acetate and limestone and (b) Ca-Mg mixed acetate and dolomite. Calcination at 900ºC (70% CO_2/30% air vol/vol) for 5 minutes, carbonation at 650ºC (15% CO_2/85% air vol/vol) for 5 minutes and recarbonation at 800ºC (90% CO_2/10% air vol/vol) for 3 minutes. "I" indicates the fast reaction-controlled phase and "II" the slow solid-state diffusion-controlled phase. In the case of limestone calcination was carried out at 950ºC to achieve full decarbonation from the 1st cycle.

20

493 Let us analyse in further detail the relative contribution of the FR and SD carbonation

494 phases to the overall CaO conversion along the carbonation/calcination cycles and how it

495 is affected by the introduction of a recarbonation stage. CaO conversion is defined as the

496 ratio of CaO mass converted to $CaCO_3$ at the end of the carbonation stage to the mass of

497 CaO before carbonation. In the case of limestone derived sorbents, conversion is simply

498 calculated by multiplying the capture capacity by the factor W_{CaO}/W_{CO_2}, where W_{CaO} and

499 W_{CO_2} are the molecular weights of CaO and CO_2 respectively. For the dolomite derived

500 sorbents, CaO conversion is calculated by multiplying the capture capacity by

501 $(1+W_{MgO}/W_{CaO})(W_{CaO}/W_{CO_2})$, where W_{MgO} is the molecular weight of MgO.

502 The separated contributions of the FR and SD phases to the overall CaO conversion, as

503 derived from the experimental thermograms, are shown in Figure 11 as a function of the

504 cycle number for the sorbents derived from the acetates. CaO conversion data in the FR

505 and SD phases are plotted in Figure 12 for the sorbents directly derived from limestone

506 (Figures 12a and 12b) and dolomite calcination (Figures 12c and 12d).

507 In general, it may be seen that CaO conversion in the FR phase is relatively small as

508 compared to conversion in the SD phase. As reported in previous works [10-11],

509 calcination under high CO_2 partial pressure yields a highly sintered CaO structure with a

510 quite reduced surface area available for fast reaction controlled carbonation, which

511 severely hampers carbonation in this initial phase. On the other hand, the diffusion

512 controlled stage is relatively promoted. The relative importance of SD carbonation is a

513 relevant point to assess the influence of solids residence time in the carbonator on the

514 capture efficiency when the CaL process is integrated into a coal fired power plant as

515 demonstrated in [44]. It must be reminded that most carbonator modelling studies use

516 data derived from thermogravimetric analyses in which the sorbents are regenerated by

517 calcination under unrealistic low CO_2 partial pressure, which leads to negligible

518 carbonation in the SD phase during the first cycles in clear contrast with our observations

519 [14].
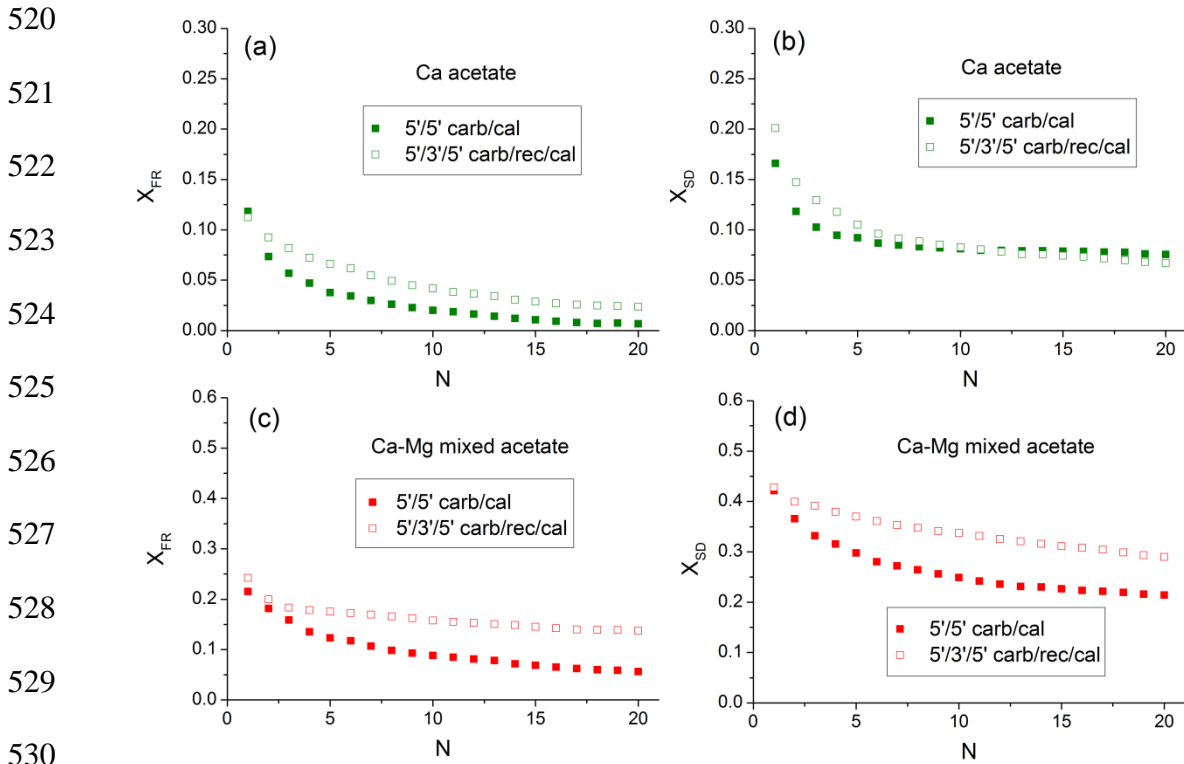
Figure 11. CaO conversion in the fast reaction controlled phase (a and c) and in the solid-state diffusion controlled phase (b and d) versus the cycle number for the sorbents derived from Ca acetate and Ca-Mg mixed acetate as indicated. Calcination at 900ºC (70% CO_2/30% air vol/vol) for 5 minutes, carbonation at 650ºC (15% CO_2/85% air vol/vol) for 5 minutes and, when introduced, recarbonation at 800ºC (90% CO_2/10% air vol/vol) for 3 minutes.

As regards the effect of recarbonation, Figures 11a-b show that, for the Ca acetate, the slight gain of CaO conversion is mainly due to the promotion of carbonation in the FR phase. In this case, recarbonation would enhance, although just moderately, the porosity of the regenerated CaO structure. The low values of CaO conversion in the FR phase for this sorbent are consistent with the marked sintering observed for CaO derived from calcium acetate in Figures 4a, 4b and 5a. The reactivation effect of recarbonation is however more evident in the case of natural limestone (Figures 12a-12b). In this case,

546
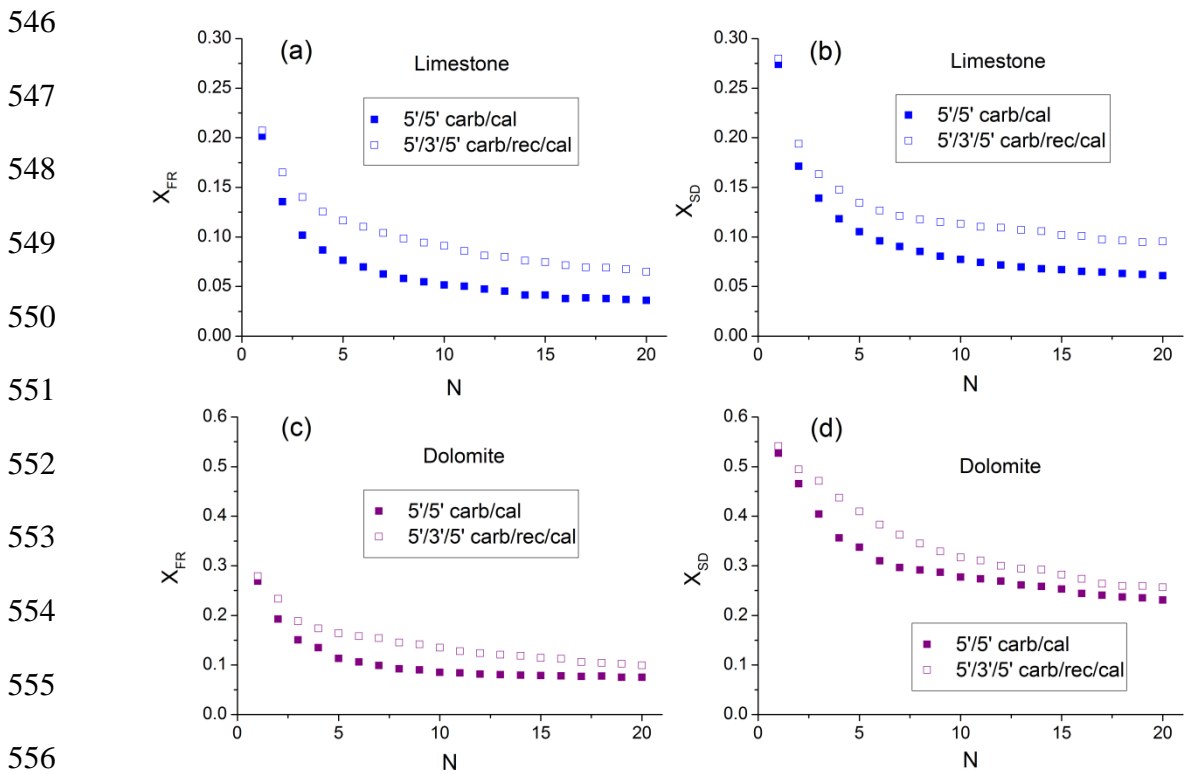
557 Figure 12. CaO conversion in the fast reaction controlled phase (a and c) and in the solid-state

558 diffusion controlled phase (b and d) versus de cycle number for the sorbents derived from

559 limestone and dolomite. Calcination at 900ºC (70% CO_2/30% air vol/vol) for 5 minutes,

560 carbonation at 650ºC (15% CO2/85% air vol/vol) for 5 minutes and, when introduced,

561 recarbonation at 800ºC (90% CO_2/10% air vol/vol) for 3 minutes as indicated. Limestone

562 calcination was carried out at 950ºC to achieve full decarbonation from the 1st cycle.

563

564 The enhancement of CaO conversion in the SD phase is more marked for the sorbents

565 derived from dolomite (Figures 11c-11d and 12c-12d) as compared to limestone. In these

566 cases, the presence of MgO inert grains in the solid structure would favor ion diffusion

567 as may be inferred from the work of Anderson [51-52], who measured by isotope

568 exchange diffusion coefficients two orders of magnitude larger in dolomite than the

569 values in calcite. Note also that the recarbonation stage causes for dolomite an increase

570 of CaO conversion in the SD phase, which is marked for the Ca-Mg mixed acetate (Figure

571 11d). Moreover, deactivation in the FR phase is notably mitigated for this sorbent by the

572 introduction of a recarbonation stage (Figure 11c).
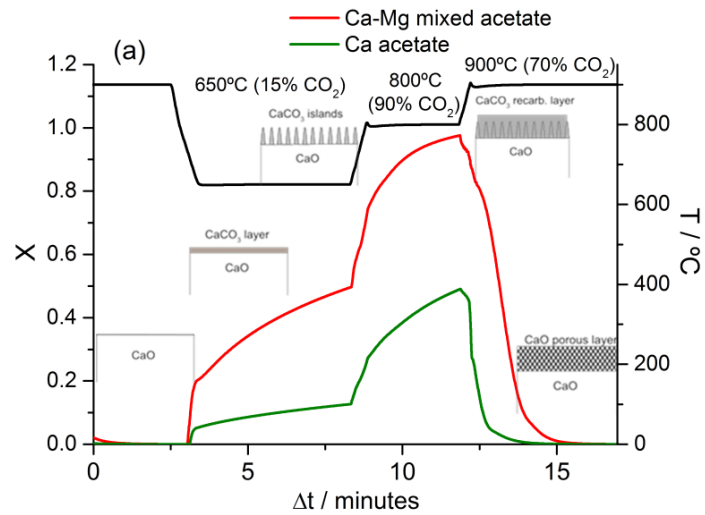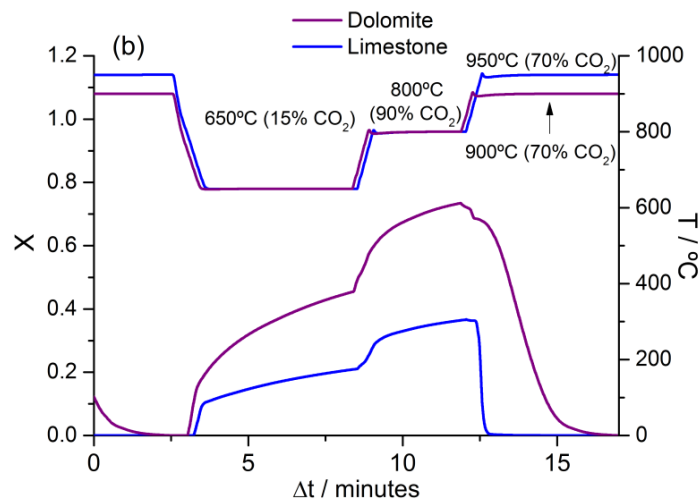
Figure 13. Time evolution of CaO conversion during the 5 minutes of carbonation, 3 minutes recarbonation and 5 minutes calcination at the 10th cycle for (a) Ca acetate and the Ca-Mg mixed acetate and (b) Limestone and dolomite. Carbonation at 650°C (15% CO_2/85% air vol/vol), recarbonation at 800°C (90% CO_2/10% air vol/vol) and calcination at 900°C (70% CO_2/30% air vol/vol). Limestone calcination was carried out at 950°C to achieve full decarbonation from the 1st cycle. A schematic representation of carbonate layer growth is also shown in a).

Figure 13a shows the time evolution of CaO conversion during the 5 minutes carbonation, 3 minutes recarbonation and 5 minutes calcination stages at the 10th cycle for the sorbents

24

596   derived from Ca acetate and the Ca-Mg mixed acetate. A schematic representation of the

597   changes in the CaO product layer morphology is also shown as was inferred elsewhere

598   by combining TGA and atomic force microscopy (AFM) using natural limestone [53-54].

599   According to this study, the $CaCO_3$ layer on the CaO surface would grow in the form of

600   islands of height depending on surface diffusion. The raise of temperature at the

601   beginning of the recarbonation stage leads to a sudden increase of surface diffusion,

602   which allows the development of higher $CaCO_3$ islands while their density decreases.

603   This leaves additional free CaO surface available for fast reaction controlled carbonation

604   under high CO_2 partial pressure, and thereby leads to a significant growth of the $CaCO_3$

605   product layer. Thus, when the sorbent is regenerated by calcination after recarbonation,

606   the thick carbonate layer would yield a CaO structure with relatively higher porosity and

607   therefore enhanced surface area. This is the fundamental mechanism by which

608   recarbonation is thought to promote the activity of the sorbent in the subsequent cycle.

609   As seen in Figure 13, our results indicate that recarbonation is enhanced for the dolomite

610   derived sorbents, which supports the idea that promoted carbonation in this stage is ruled

611   by surface diffusion that would be favored by the presence of MgO inert domains. This

612   is specially marked in the case of the Ca-Mg mixed acetate (Figure 13a), which suggests

613   that the treatment with acetic acid would mitigate segregation of the MgO grains. This

614   would explain also why deactivation of the Ca-Mg acetate derived sorbent is reduced as

615   obtained from the multicycle capture capacity data (Figure 9b). In agreement with this

616   argument, Figure 14 shows SEM micrographs of Ca-Mg mixed acetate and dolomite

617   samples after being subjected to carbonation/recarbonation/calcination cycles in which

618   segregation of MgO and CaO grains is more apparent in the case of dolomite.

619

620
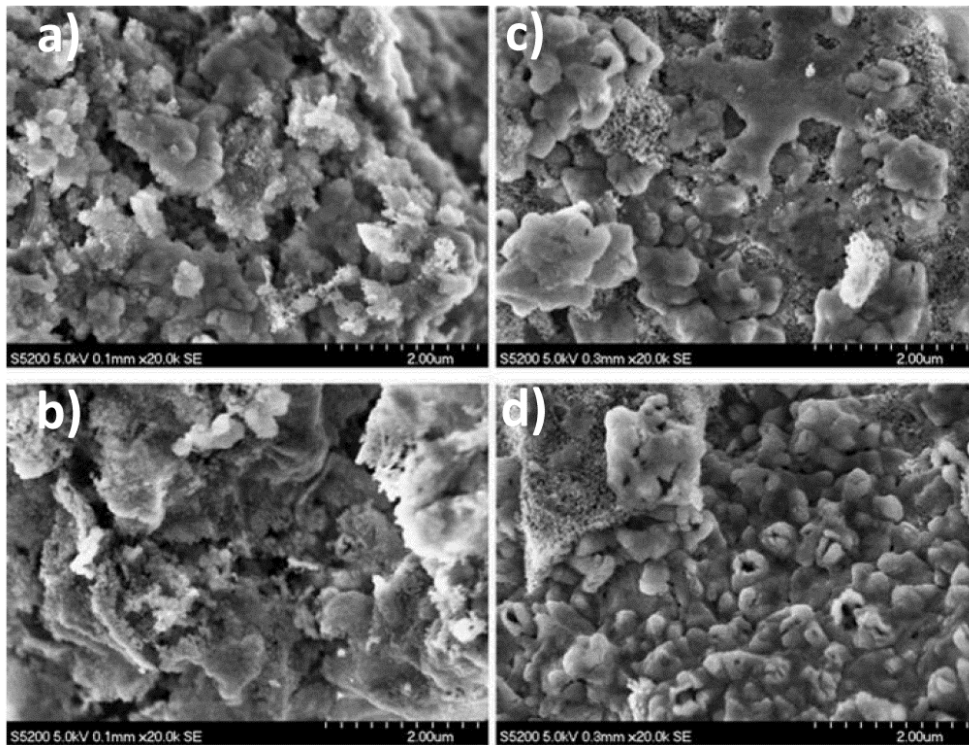
Figure 14. SEM pictures of Ca-Mg mixed acetate (a,b) and dolomite samples (c,d) after being subjected to 20 carbonation/recarbonation/calcination cycles. Carbonation at 650ºC (15% CO_2/85% air vol/vol), recarbonation at 800ºC (90% CO_2/10% air vol/vol) and calcination at 900ºC (70% CO_2/30% air vol/vol).

4. Conclusions

In this work, the multicycle CO_2 capture performance of CaO derived from Ca and Ca-Mg mixed acetates obtained from acetic acid treatment of limestone and dolomite, respectively, has been studied at realistic Ca-Looping conditions. These necessarily involve calcination under high CO_2 partial pressure and fast transitions between carbonation and calcination stages.

Acetic acid treatment of limestone produces almost pure Ca acetate, with a minor amount of Ca-Mg acetate. On the other hand, acetic acid treatment of dolomite leads to a Ca-Mg

647   mixed acetate consisting of a mixture of Ca-Mg acetate and Ca acetate. Acetic acid

648   pretreatment of limestone allows for a higher calcination efficiency at reduced

649   temperatures (900ºC) as compared to natural limestone (>930ºC) due to the relatively low

650   crystallinity of the $CaCO_3$ derived from Ca acetate decomposition as compared to

651   limestone. On the other hand, acetic acid pretreatment of limestone and dolomite does not

652   lead to an improvement of their capture capacity under carbonation/calcination cycles,

653   which is against previous results mostly obtained under CaL conditions involving

654   unrealistically low CO_2 partial pressure in the calcination stage for sorbent regeneration.

655   Yet, the results obtained also demonstrate that a significantly high residual capture

656   capacity ($CC_r = 0.168$) is obtained for the Ca-Mg mixed acetate if a recarbonation stage

657   is introduced as compared to natural dolomite ($CC_r = 0.088$). The main reason for this

658   behavior is the enhancement of carbonation in the solid-state diffusion controlled phase,

659   which confers a relevant role to the solids residence time in the carbonator on the CO_2

660   capture efficiency. Moreover, the progressive segregation of the MgO and CaO grains

661   with the number of cycles is reduced in the case of the Ca-Mg mixed acetate as compared

662   with dolomite, which helps mitigating sorbent deactivation.

663

664

672 Services of the Innovation, Technology and Research Centre of the University of Seville

673 (CITIUS).

674

675

676 **6. References**

677 [1]   A. Perejón, L.M. Romeo, Y. Lara, P. Lisbona, A. Martínez, J.M. Valverde, The

678   calcium-looping technology for CO_2 capture: On the important roles of energy

679   integration and sorbent behavior, Applied Energy 162 (2015) 787-807.

680   10.1016/j.apenergy.2015.10.121.

681 [2]   D.P. Hanak, E.J. Anthony, V. Manovic, A review of developments in pilot-plant

682   testing and modelling of calcium looping process for CO_2 capture from power

683   generation systems, Energy & Environmental Science 8 (2015) 2199-2249.

684   10.1039/C5EE01228G.

685 [3]   J. Blamey, E.J. Anthony, J. Wang, P.S. Fennell, The calcium looping cycle for

686   large-scale CO_2 capture, Progress in Energy and Combustion Science 36 (2010)

687   260-279. http://dx.doi.org/10.1016/j.pecs.2009.10.001.

688 [4]   J.M. Valverde, Ca-Based synthetic materials with enhanced CO_2 capture

689   efficiency, J. Mater. Chem. A 1 (2013) 447-468. 10.1039/c2ta00096b.

690 [5]   M.C. Romano, Modeling the carbonator of a Ca-Looping process for CO_2 capture

691   from power plant flue gas, Chem. Eng. Sci. 69 (2012) 257-269.

692   10.1016/j.ces.2011.10.041.

693 [6]   R.S. Middleton, J.K. Eccles, The complex future of CO_2 capture and storage:

694   Variable electricity generation and fossil fuel power, Applied Energy 108 (2013)

695   66-73. http://dx.doi.org/10.1016/j.apenergy.2013.02.065.

696   [7]   D.J. Roddy, Development of a CO_2 network for industrial emissions, Applied
697   Energy 91 (2012) 459-465. http://dx.doi.org/10.1016/j.apenergy.2011.10.016.

698   [8]   A. Martínez, Y. Lara, P. Lisbona, L.M. Romeo, Operation of a cyclonic preheater
699   in the Ca-Looping for CO_2 capture, Environmental Science & Technology 47
700   (2013) 11335-11341. 10.1021/es401601k.

701   [9]   A. Martínez, Y. Lara, P. Lisbona, L.M. Romeo, Operation of a mixing seal valve
702   in calcium looping for CO_2 capture, Energy & Fuels 28 (2014) 2059-2068.
703   10.1021/ef402487e.

704   [10]   J.M. Valverde, P.E. Sanchez-Jimenez, L.A. Perez-Maqueda, Limestone
705   calcination nearby equilibrium: Kinetics, CaO crystal structure, sintering and
706   reactivity, Journal of Physical Chemistry C 119 (2015) 1623-1641.
707   10.1021/jp508745u.

708   [11]   J.M. Valverde, P.E. Sanchez-Jimenez, A. Perejon, L.A. Perez-Maqueda, CO_2
709   multicyclic capture of pretreated/doped CaO in the Ca-Looping process. Theory
710   and experiments, Phys. Chem. Chem. Phys. 15 (2013) 11775-11793.
711   10.1039/c3cp50480h.

712   [12]   C. Ortiz, R. Chacartegui, J.M. Valverde, J.A. Becerra, L.A. Perez-Maqueda, A
713   new model of the carbonator reactor in the calcium looping technology for post-
714   combustion CO_2 capture, Fuel 160 (2015) 328-338. 10.1016/j.fuel.2015.07.095.

715   [13]   J.C. Abanades, E.J. Anthony, D.Y. Lu, C. Salvador, D. Alvarez, Capture of CO_2
716   from Combustion Gases in a Fluidized Bed of CaO, AIChE Journal 50 (2004)
717   1614-1622. 10.1002/aic.10132.

718   [14]   J.M. Valverde, P.E. Sanchez-Jimenez, L.A. Perez-Maqueda, Role of
719   precalcination and regeneration conditions on postcombustion CO_2 capture in the

720   Ca-Looping technology, Applied Energy 136 (2014) 347-356.
721   10.1016/j.apenergy.2014.09.052.

722 [15] B. Arias, G.S. Grasa, M. Alonso, J.C. Abanades, Post-Combustion calcium
723   looping process with a highly stable sorbent activity by recarbonation, Energy &
724   Environmental Science 5 (2012) 7353-7359. 10.1039/C2EE03008J.

725 [16] L.M. Romeo, Y. Lara, P. Lisbona, A. Martínez, Economical assessment of
726   competitive enhanced limestones for CO_2 capture cycles in power plants, Fuel
727   Processing Technology 90 (2009) 803-811.
728   http://dx.doi.org/10.1016/j.fuproc.2009.03.014.

729 [17] J.M. Valverde, P.E. Sanchez-Jimenez, L.A. Perez-Maqueda, Ca-Looping for
730   postcombustion CO_2 capture: A comparative analysis on the performances of
731   dolomite and limestone, Applied Energy 138 (2015) 202-215.
732   10.1016/j.apenergy.2014.10.087.

733 [18] P.E. Sanchez-Jimenez, L.A. Perez-Maqueda, J.M. Valverde, Nanosilica
734   supported CaO: A regenerable and mechanically hard CO_2 sorbent at Ca-Looping
735   conditions, Applied Energy 118 (2014) 92-99. 10.1016/j.apenergy.2013.12.024.

736 [19] A.M. Kierzkowska, R. Pacciani, C.R. Müller, CaO-based CO_2 sorbents: from
737   fundamentals to the development of new, highly effective materials,
738   ChemSusChem 6 (2013) 1130-1148. 10.1002/cssc.201300178.

739 [20] H. Lu, E.P. Reddy, P.G. Smirniotis, Calcium oxide based sorbents for capture of
740   carbon dioxide at high temperatures, Industrial & Engineering Chemistry
741   Research 45 (2006) 3944-3949. 10.1021/ie051325x.

742 [21] Y.J. Li, C.S. Zhao, H.C. Chen, Y.K. Liu, Enhancement of Ca-based sorbent
743   multicyclic behavior in ca looping process for CO_2 separation, Chem. Eng.
744   Technol. 32 (2009) 548-555. 10.1002/ceat.200800525.

745 [22] Y. Li, C. Zhao, H. Chen, Q. Ren, L. Duan, CO_2 capture efficiency and energy

746 requirement analysis of power plant using modified calcium-based sorbent

747 looping cycle, Energy 36 (2011) 1590-1598.

748 http://dx.doi.org/10.1016/j.energy.2010.12.072.

749 [23] H. Lu, A. Khan, P.G. Smirniotis, Relationship between structural properties and

750 CO_2 capture performance of CaO−based sorbents obtained from different

751 organometallic precursors, Industrial & Engineering Chemistry Research 47

752 (2008) 6216-6220. 10.1021/ie8002182.

753 [24] Y.J. Li, R.Y. Sun, H.L. Liu, C.M. Lu, Cyclic CO_2 capture behavior of limestone

754 modified with pyroligneous acid (PA) during calcium looping cycles, Industrial

755 & Engineering Chemistry Research 50 (2011) 10222-10228. 10.1021/ie2007455.

756 [25] Y.J. Li, C.S. Zhao, L.B. Duan, C. Liang, Q.Z. Li, W. Zhou, H.C. Chen, Cyclic

757 calcination/carbonation looping of dolomite modified with acetic acid for CO_2

758 capture, Fuel Processing Technology 89 (2008) 1461-1469.

759 10.1016/j.fuproc.2008.07.008.

760 [26] L. Li, D.L. King, Z. Nie, C. Howard, Magnesia-Stabilized Calcium Oxide

761 Absorbents with Improved Durability for High Temperature CO2 Capture,

762 Industrial & Engineering Chemistry Research 48 (2009) 10604-10613.

763 10.1021/ie901166b.

764 [27] X. Ma, Y. Li, L. Shi, Z. He, Z. Wang, Fabrication and CO2 capture performance

765 of magnesia-stabilized carbide slag by by-product of biodiesel during calcium

766 looping process, Applied Energy 168 (2016) 85-95.

767 http://dx.doi.org/10.1016/j.apenergy.2016.01.080.

768   [28]   C. Chi, Y. Li, R. Sun, X. Ma, L. Duan, Z. Wang, HCl removal performance of

769   Mg-stabilized carbide slag from carbonation/calcination cycles for CO2 capture,

770   RSC Advances 6 (2016) 104303-104310. 10.1039/C6RA19972K.

771   [29]   D.S. Sultan, C.R. Müller, J.S. Dennis, Capture of CO2 Using Sorbents of Calcium

772   Magnesium Acetate (CMA), Energy & Fuels 24 (2010) 3687-3697.

773   10.1021/ef100072q.

774   [30]   C. Luo, Y. Zheng, Y. Xu, N. Ding, Q. Shen, C. Zheng, Wet mixing combustion

775   synthesis of CaO-based sorbents for high temperature cyclic CO2 capture, Chem.

776   Eng. J. 267 (2015) 111-116. http://dx.doi.org/10.1016/j.cej.2015.01.005.

777   [31]   R. Filitz, A.M. Kierzkowska, M. Broda, C.R. Müller, Highly Efficient CO2

778   Sorbents: Development of Synthetic, Calcium-Rich Dolomites, Environmental

779   Science & Technology 46 (2012) 559-565. 10.1021/es2034697.

780   [32]   D. Lu, R. Hughes, E. Anthony, V. Manovic, Sintering and reactivity of $CaCO_3$ -

781   based sorbents for in situ CO_2 capture in fluidized beds under realistic calcination

782   conditions, Journal of Environmental Engineering 135 (2009) 404-410.

783   10.1061/(ASCE)EE.1943-7870.0000079.

784   [33]   J.M. Valverde, P.E. Sanchez-Jimenez, A. Perejon, L.A. Perez-Maqueda, Role of

785   looping-calcination conditions on self-reactivation of thermally pretreated CO_2

786   sorbents based on CaO, Energy & Fuels 27 (2013) 3373-3384.

787   10.1021/ef400480j.

788   [34]   N. Koga, J.M. Criado, The influence of mass transfer phenomena on the kinetic

789   analysis for the thermal decomposition of calcium carbonate by constant rate

790   thermal analysis (CRTA) under vacuum, International Journal of Chemical

791   Kinetics 30 (1998) 737-744. 10.1002/(SICI)1097-4601(1998)30:10<737::AID-

792   KIN6>3.0.CO;2-W.

793   [35]   J. Panzer, Nature of calcium acetate, Journal of Chemical & Engineering Data 7

794   (1962) 140-142. 10.1021/je60012a040.

795   [36]   H.E. Todd, D.L. Walters, United States Patent, 1990.

796   [37]   J. Adanez, L.F. de Diego, F. Garcia-Labiano, Calcination of Calcium Acetate and

797   Calcium Magnesium Acetate: Effect of the Reacting Atmosphere, Fuel 78 (1999)

798   583-592. 10.1016/s0016-2361(98)00186-0.

799   [38]   D.H. Han, H.Y. Sohn, Calcined calcium magnesium acetate as a superior SO_2

800   sorbent: I. Thermal decomposition, Aiche Journal 48 (2002) 2971-2977.

801   10.1002/aic.690481222.

802   [39]   A.W. Musumeci, R.L. Frost, E.R. Waclawik, A spectroscopic study of the mineral

803   paceite (calcium acetate), Spectrochimica Acta Part A: Molecular and

804   Biomolecular Spectroscopy 67 (2007) 649-661.

805   http://dx.doi.org/10.1016/j.saa.2006.07.045.

806   [40]   J. Steciak, Y.A. Levendis, D.L. Wise, Effectiveness of calcium magnesium

807   acetate as dual SO_2 -NO_x emission control agent, AIChE Journal 41 (1995) 712-

808   722. 10.1002/aic.690410328.

809   [41]   M. Broda, A.M. Kierzkowska, C.R. Muller, Development of highly effective

810   CaO-based, MgO-stabilized CO_2 sorbents via a scalable "One-Pot"

811   recrystallization technique, Advanced Functional Materials 24 (2014) 5753-5761.

812   10.1002/adfm.201400862.

813   [42]   J.M. Valverde, A. Perejon, S. Medina, L.A. Perez-Maqueda, Thermal

814   decomposition of dolomite under CO_2: Insights from TGA and in situ XRD

815   analysis, Phys. Chem. Chem. Phys. 17 (2015) 30162-30176.

816   10.1039/c5cp05596b.

817   [43]   P.E. Sanchez-Jimenez, J.M. Valverde, A. Perejon, A. de la Calle, S. Medina, L.A.

818   Perez-Maqueda, Influence of Ball Milling on CaO Crystal Growth During

819   Limestone and Dolomite Calcination: Effect on CO2 Capture at Calcium Looping

820   Conditions, Cryst. Growth Des. 16 (2016) 7025-7036. 10.1021/acs.cgd.6b01228.

821   [44]   C. Ortiz, R. Chacartegui, J.M. Valverde, J.A. Becerra, A new integration model

822   of the calcium looping technology into coal fired power plants for CO_2 capture,

823   Applied   Energy   169   (2016)   408-420.

824   http://dx.doi.org/10.1016/j.apenergy.2016.02.050.

825   [45]   G.S. Grasa, J.C. Abanades, CO_2 capture capacity of CaO in long series of

826   carbonation/calcination cycles, Industrial & Engineering Chemistry Research 45

827   (2006) 8846-8851. 10.1021/ie0606946.

828   [46]   J.M. Valverde, A model on the CaO multicyclic conversion in the Ca-Looping

829   process, Chem. Eng. J. 228 (2013) 1195-1206. 10.1016/j.cej.2013.05.023.

830   [47]   R. Barker, The reversibility of the reaction $CaCO_3 \rightleftarrows CaO+CO_2$, Journal of

831   Applied   Chemistry   and   Biotechnology   23   (1973)   733-742.

832   10.1002/jctb.5020231005.

833   [48]   G. Grasa, R. Murillo, M. Alonso, J.C. Abanades, Application of the random pore

834   model to the carbonation cyclic reaction, AIChE Journal 55 (2009) 1246-1255.

835   10.1002/aic.11746.

836   [49]   Z. Li, Y. Liu, N. Cai, Understanding the enhancement effect of high-temperature

837   steam on the carbonation reaction of CaO with CO_2, Fuel 127 (2014) 88-93.

838   http://dx.doi.org/10.1016/j.fuel.2013.06.040.

839   [50]   M. Alonso, N. Rodríguez, G. Grasa, J.C. Abanades, Modelling of a fluidized bed

840   carbonator reactor to capture CO_2 from a combustion flue gas, Chem. Eng. Sci.

841   64 (2009) 883-891. http://dx.doi.org/10.1016/j.ces.2008.10.044.

842   [51]   T.F. Anderson, Self-Diffusion of carbon and oxygen in calcite by isotope
843   exchange with carbon dioxide, Journal of Geophysical Research 74 (1969) 3918-
844   3932. 10.1029/JB074i015p03918.

845   [52]   T.F. Anderson, Self-Diffusion of carbon and oxygen in dolomite, Journal of
846   Geophysical Research 77 (1972) 857-861. 10.1029/JB077i005p00857.

847   [53]   Z. Li, H. Sun, N. Cai, Rate equation theory for the carbonation reaction of CaO
848   with CO_2, Energy & Fuels 26 (2012) 4607-4616. 10.1021/ef300607z.

849   [54]   Z.-s. Li, F. Fang, X.-y. Tang, N.-s. Cai, Effect of temperature on the carbonation
850   reaction of CaO with CO_2, Energy & Fuels 26 (2012) 2473-2482.
851   10.1021/ef201543n.

852